

The Lithium Wall Stellarator Experiment in TJ-II

Francisco L. TABARÉS, David TAFALLA, Jose A. FERREIRA, Maria A OCHANDO, Francisco MEDINA, Enrique ASCASIBAR, Teresa ESTRADA, Candida FUENTES, Isabel GARCÍA-CORTÉS, Jose GUASP, Macarena LINIERS, Ignacio PASTOR, Maria A. PEDROSA and the TJ-II Team*

Laboratorio Nacional de Fusión. CIEMAT. Avenida Complutense 22, 28040 Madrid, Spain

(Received 23 January 2009 / Accepted 14 July 2009)

In the last years, lithium wall conditioning has been carried out in several fusion devices by different techniques, providing in many instances record values of plasma parameters and enhanced plasma reproducibility and opening the possibility of developing high radiative, low recycling liquid divertor concepts of high potential for future reactors. This concept has been termed the Li Tokamak Reactor. Compared to tokamaks, stellarator plasmas show distinct features in their interaction with the surrounding materials. The lack of disruptions and type I ELMs make them more reliable for reactor operation. So it is the lack of MHD-driven density limit. On the other side, the intrinsic radiative character of the density limit of stellarators and the tendency to central impurity accumulation makes wall-material selection paramount. In the present work, the plasma performance of the TJ-II Helic under Li-coated wall conditions is described. Compared to previous coatings, lithium has produced the best plasma performance to date, leading to the achievement of record values in plasma density and energy confinement. Plasma profiles free from impurity accumulation have been obtained under specific fuelling schemes. Future research lines in this direction, with impact on the design of a Li stellarator reactor concept, are also addressed.

© 2010 The Japan Society of Plasma Science and Nuclear Fusion Research

Keywords: lithium, stellarator, fusion reactor, first wall material, recycling, impurity accumulation, TJ-II

DOI: 10.1585/pfr.5.S1012

1. Introduction

Plasma wall interaction issues are paramount in achieving fusion plasmas with high purity, controlled density and high confinement. Even when the selection of plasma facing components, such as limiter and divertor target materials, is made based on their ability to withstand the very high particle and power fluxes that are characteristic of present fusion plasmas, the interaction with the first wall, reached by charge exchange neutrals, photons and some more or less tenuous plasma, is considered to contribute to the plasma impurity content as much as the wetted areas do. Therefore, a growing concern about proper conditioning of the total inner wall of the fusion device has been taking place in the last decades.

Compared to tokamaks, stellarator plasmas show distinct features in their interaction with the surrounding materials. On the good side, the lack of disruptions and type I ELMs make the choice of plasma facing components less demanding. In addition, the lack of MHD-driven density limit [1] has allowed their operation at densities well above the corresponding Greenwald limit for tokamaks [2, 3]. Since plasma collapse in stellarators seems to be mainly governed by local power balance considerations [4], changes in wall materials are ideally suited for the vali-

ation of the running models for the density limit in these devices. As a potential drawback, neoclassical transport characteristics of the core plasma in stellarators make them prone to impurity accumulation [5], thus stressing the use of low Z elements as PFC. Although some specific divertor concepts have been developed for stellarator with reasonable success for impurity and particle control [6], no particular coating strategies for the first wall have been developed. As one could expect, the application of those concepts with good performance in tokamaks, such as boronization or Ti gettering, has also improved machine operation in the stellarator community [7]. A closed coupling between the divertor efficiency and the recycling characteristics of the wall has been recently evidenced in LHD, as shown by the achievement of the IDB-SDC mode in the absence of the LID operation, only under low recycling wall conditions [8]. Therefore, low Z , low recycling first wall scenarios look highly promising if a stellarator reactor concept is to be developed.

Among the available low Z coating options (Be, C and B) lithium is a very attractive element due to its very low radiation power, strong H retention and strong O getter activity and excellent results have been achieved recently in tokamaks [9–11]. Also, and in direct connection to the lower recycling scenario leading to decreased CX losses and higher temperatures, important changes in energy con-

author's e-mail: tabares@ciemat.es

*See author list in ref. 14

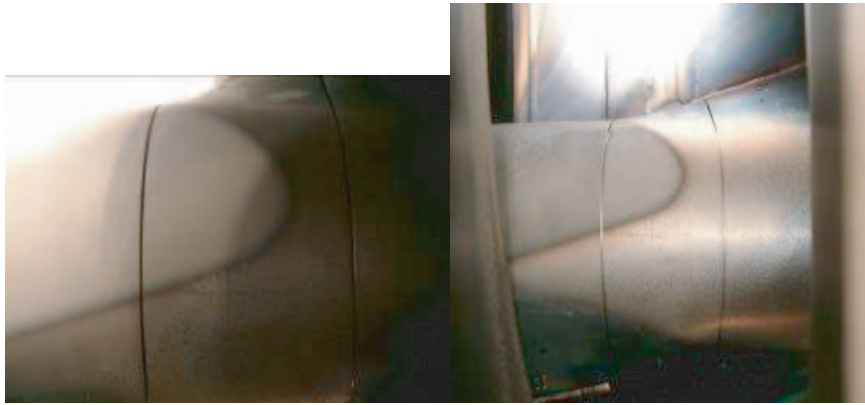


Fig. 1 Initial (left) and redistributed (right) lithium deposit on the grooved part of the vacuum vessel of TJ-II.

finement have been predicted [12] and observed [13]. In the present work, the operation of a stellarator, the TJ-II Helic [14], with lithium-coated walls is described and compared to previous wall coating conditions. The most relevant changes on the plasma performance and confinement characteristics associated to the new wall scenario are described and analyzed in terms of enhanced impurity and particle control.

2. Coating Technique

The TJ-II stellarator has been operated under different first wall conditions since its beginning [15] and details about the applied techniques and resulting plasma performance can be found in the proceedings of the recent 18th PSI conference [16]. Basically, under ECR plasma generation and heating, the density control is hampered by the combination of low cut-off density ($n_e(0) < 1.7 \times 10^{19} \text{ m}^{-3}$) and the fast saturation of the small ($\sim 0.5 \text{ m}^2$ vs. $\sim 40 \text{ m}^2$) plasma-interacting surface located at the grooved wall area which surrounds the two characteristic central coils. Another factor in play is the presence of the Enhanced Particle Confinement (EPC) mode, characterized by a sudden increase of particle confinement at a critical line average density in the order of $0.6 \times 10^{19} \text{ m}^{-3}$ [17]. Transition to this mode, was found to strongly depend on fuelling pulse shape and amplitude and its development can be eventually suppressed by proper tailoring of the gas puffing. The transition to the EPC mode is correlated with the development of edge-sheared flows [18].

In the 2007-08 experimental campaign, a low recycling, low Z wall has been tested. For that purpose, an *in situ* lithium coating technique (herein referred as lithiation) was developed. It is based on evaporation under vacuum from four ovens, symmetrically spaced and oriented tangentially to the vacuum vessel in the equatorial plane of the machine. A total of 4 g of metallic Li is evaporated during each conditioning cycle, at temperatures of 500-600 °C. Effusion from the ovens creates an atomic beam aiming at the remote region opposed to the corresponding flange.

Under HV operation, the mean free path of the Li atoms is long enough to produce a thin layer at the vessel walls located midway between adjacent ovens. The initial deposition pattern, directly visible in the groove protecting the central coils, matches the line of sight flight of the Li atoms. However, plasma operation was found to redistribute the initial coating very efficiently and the beneficial effect of the coating extended far beyond that expected from the localized deposition (Fig. 1). Nevertheless, in order to extend the lifetime of the Li coating, and due to the very high reactivity of this species with background gases (water, O_2 , N_2 , $\text{CO} \dots$) a $\sim 50 \text{ nm}$ boron layer was deposited by glow discharge in a He/o-carborane mixture prior to the evaporation (see [15] for more details). A He GD depleted the H from the B coating after its deposition. Also, He GD was applied every day on the Li layer in order to remove hydrogen from the areas not fully covered by the coating. A total of 12 g of Li were evaporated for the ~ 1000 discharges performed in this period. All these coating and conditioning procedures were applied over the vacuum vessel stainless steel walls, at room temperature. No heating of the walls was applied either during normal plasma operation.

3. Particle Confinement

The most remarkable change upon lithiation of TJ-II was a conspicuous improvement of particle control by external puffing compared to the former, B-coated scenario. Not only the required puffing levels were significantly higher, by a factor of 2-3, to obtain the same density (feed-forward operation mode), but also no sign of wall saturation was observed after a full day of ECRH operation. Particle balance measurements under the Li coated walls yields a total retention $\sim 4 \times 10^{21} \text{ H/m}^2$ after one day of operation ($\sim 45, 200 \text{ ms}$ discharges), a factor 5 higher than the B wall saturation limit at room temperature, which takes place at total retained inventory of $\sim 8 \times 10^{20} \text{ H/m}^2$ (RT values). Even assuming that a full H/Li ratio of 1 was achieved (thus implying the stoichiometry of the hy-

drude), a depth of ~ 80 nm will be saturated. This is much higher than the expected implantation range of 100's eV protons. Of particular relevance on machine performance is the recovery of pumping walls characteristics after shots with densities above cut-off. Typically, one or two purges (dry discharges) were required in B scenarios. However, no such a need was found upon lithiation, the wall memory effect being basically washed out, i.e., a slight decrease of pre-programmed puffing rate was enough for achieving controlled densities after the production of a cut-off event. All these observations concerning wall inventory under Li walls point to strong diffusion of the implanted H into the wall coating, which may be different from the initially deposited one after plasma operation.

The dynamic behavior of plasma particles for H and He plasmas was investigated by perturbative experiments. A value of the effective confinement time, $t_p/(1 - R)$, of ~ 8 ms were deduced for H plasmas in freshly deposited

Li. Assuming no major changes in particle confinement respect to the boron and metal cases [19], a value of $R < 0.20$ is obtained. Note that this low value still reflects the limited extension of the wall coverage by the Li coating achieved and it is therefore prone to improvement. It is also worth noting that this value was slowly evolving after some hundreds of shots up to values of $R \sim 0.5$. Also shown in Fig. 2, perturbative experiments in He fuelled discharges yields a R value of ~ 0.93 . This, less than one, recycling coefficient value is in line with previous observations of He pumping in low temperature Li walls [10] and opens the possibility to selective removal of reactor fuel particles and resulting ashes.

Of special challenge in TJ-II, density control in NBI plasmas was dramatically improved by the lithium coating. Both, plasma reproducibility and density control were significantly better than in previous campaigns. As an example, Fig. 3 shows the time evolution of some character-

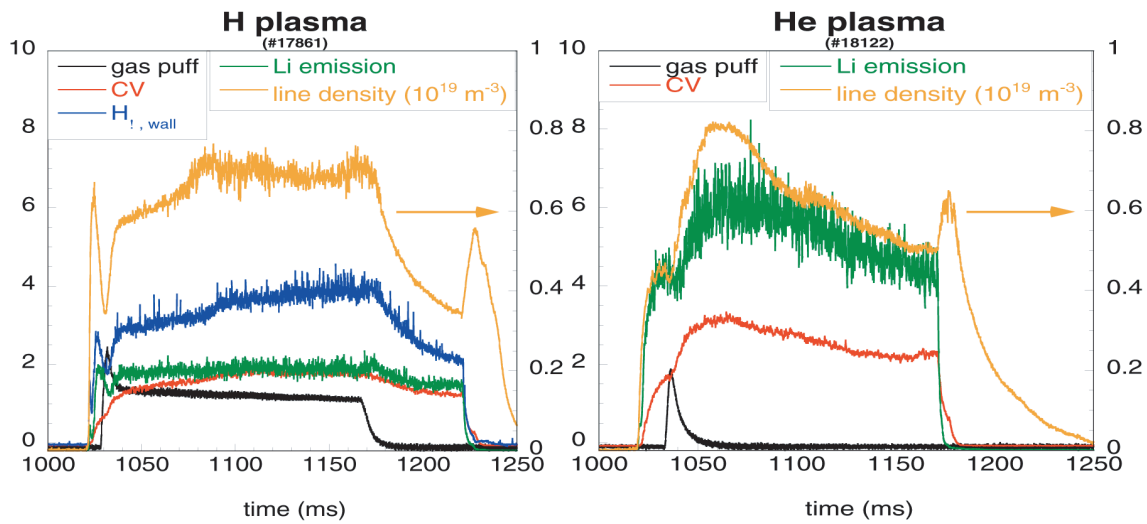


Fig. 2 Recycling characteristics of H and He plasmas under Li-wall operation.

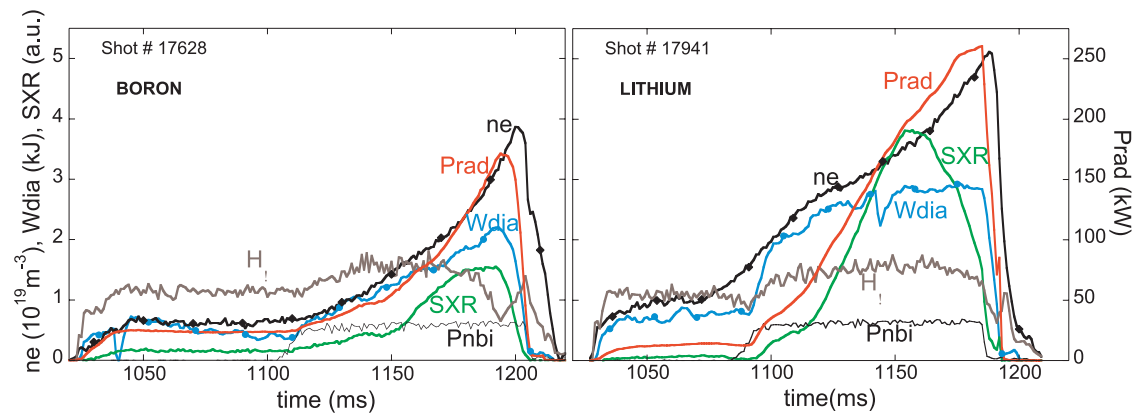


Fig. 3 Comparative time evolution of relevant plasma parameters for the B wall (left) and Li wall (right) scenarios. The injection of NB (~ 450 kW) is also displayed. $H\alpha$ values are not calibrated (a.u.).

istic parameters (line density, W diamagnetic, Soft X Ray emission, total radiated power and $H\alpha$ at the wall) for two representative examples of B and Li walls. As seen, an uncontrolled rise of electron density upon the NB injection (~ 450 kW) takes place in the B case (see Fig. 3 left), leading to a plasma collapse (roll-over of the W_{dia} , SXR and bolometer traces at 1190 ms). For the Li example (Fig. 3 right), however, a higher density can be achieved, with larger, stationary values of diamagnetic energy content, even when the high levels of radiated power represent a larger sink of the available heating power in this case. In the Fig. 3 (right), it is also worth noting that particle fluxes to the wall during the NBI phase, as monitored by the different $H\alpha$ monitors located all over the machine, remain basically at the ECRH plasma level thus indicating a strong enhancement (up to a factor of 4) of global particle confinement. This effect is also supported by the Li neutral emission signal (at 671 nm) and in the particle fluxes deduced from Langmuir probes (not shown), that precludes a possible effect of dilution of the proton content at the edge. For high particle confinement and NBI pulse length of ~ 100 ms, the density rise should be ultimately limited by the beam fuelling rate which, for a 31 keV, 0.5 MW power can be evaluated in $\sim 10^{20} e^-/s$. This value was indeed experimentally observed. Furthermore, no sign of collapse was seen up to central density values of $8 \times 10^{19} \text{ m}^{-3}$, depending on the shape of the resulting plasma profile (see below).

4. Impurity Behavior and Plasma Emissivity

Clean plasmas are routinely obtained in TJ-II ECR heated plasmas under low Z scenarios, largely due to the strong oxygen gettering effect of the B coatings and the use of graphite limiters [15]. Although the Li coatings were not aimed at improving this situation, significant effects have been observed in the last campaign: the electron density-normalized signals from carbon emission, radiated power, neutral lithium and other impurity-related signals were seen to decrease during the operation. The observations for the two first days of operation after lithiation are displayed in Fig. 4. A concomitant evolution of particle recycling towards lower levels was eventually observed. Since the initial deposition pattern of Li was found to evolve with plasma operation, spreading over the plasma-interaction area, it is supposed that a gradual improvement of the coating homogeneity by plasma erosion of the initial localized deposition region can be responsible for the observed behavior. In order to shed some light into this important point, a spectroscopic estimate of the erosion yield of Li by the plasma was made.

From the calibrated intensities of the $H\alpha$ and LiI (671 nm) lines, a yield of $(0.5-1) \times 10^{-3} \text{ Li/H}$ was deduced at several locations of the vessel. These figures are at least a factor 30 lower than expected from TRIM code [20] for

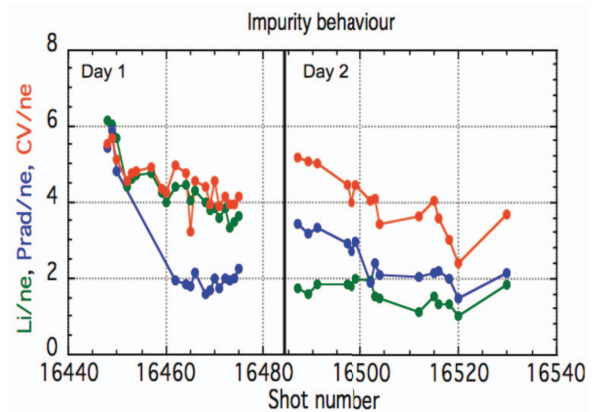


Fig. 4 Impurity evolution during the first two days after lithiation of the walls.

the calculation of the corresponding sputtering yield at the measured edge temperature of 50-60 eV and the reason of this mismatch is still under investigation. Plasma spectroscopy and soft X ray measurements, together with the IONEQ impurity transport code [21] indicate that carbon still represents the main contaminant in Li-wall scenarios. Sources of this impurity are the residual of change in carbon in the exposed boron films coming from the underlying o-carborane coating and, of special relevance in NBI, high density plasmas, the protecting graphite elements associated to the beam injection line.

As a consequence of the impurity composition and good particle confinement, total radiation levels can be higher in the Li scenarios as compared to those obtained in boronized walls. However, the development of the plasma collapse follows a different pattern in both cases. Higher densities were systematically obtained at the maximum of the diamagnetic energy content signal, W_{dia} , under Li wall operation, as can be seen in the examples given in Fig. 3. Radial profiles of radiation losses were determined from absolutely calibrated bolometer arrays located at several toroidal and poloidal locations. Two different profiles developed depending on fuelling strategy and local plasma parameters. Examples of these profiles are shown in Figure 5. For the broad, dome-type profile (on the left), central radiation levels are almost half than those observed in the peaked, bell-type counterpart (on the right). From the analysis of SXR emission profile, it is concluded that central values of Z_{eff} differ, indicating an impurity accumulation in the bell-type scenario with central Z_{eff} values up to 2.8. The radial shapes of plasma emissivity of Fig. 5 are mirrored by the Thomson Scattering data of plasma density, with central values up to $8 \times 10^{19} \text{ m}^{-3}$ in the bell-type profile and almost constant electron temperatures of 200-300 eV across the plasma minor radius. Also, atomic beam and reflectometer data yield steeper gradients in the edge region for the bell type profile.

In spite of their lower, total radiated power, development of the dome-type profile was systematically associ-

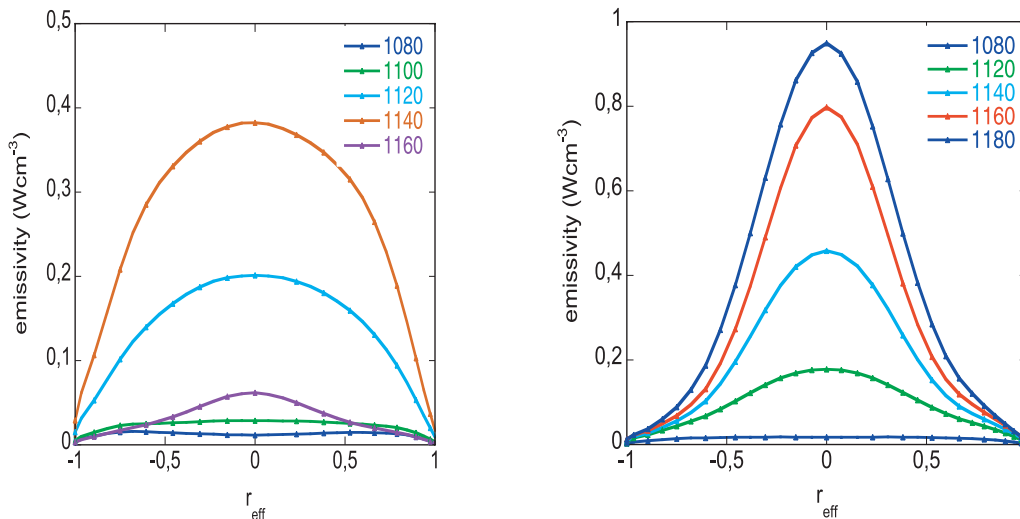


Fig. 5 Radial profiles of plasma emissivity (bolometer) for two different type of profiles obtained under Li-wall operation: left: dome type, right: bell type. Note the different central and peripheral radiation levels.

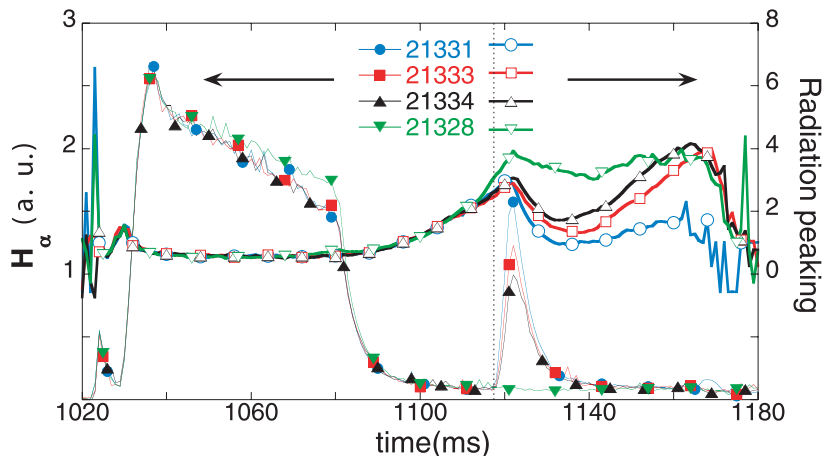


Fig. 6 Evolution of the radiation peaking factor (centre/edge, bolometer) upon injection of a H₂ pulse. From top to bottom, the amplitude of the pulse is decreasing.

ated to a prompt plasma collapse. One of the possible causes of this fact can be found in the local power balance established at the plasma edge under central heating conditions. Indeed, the data shown in Fig. 5 indicate a significantly lower radiated power at the edge for the peaked, non-collapsing profiles. This balance has been called into play in defining the density limit in stellarators through the so-called “*low-radiative collapse*” [4]. However, with the limited information presently available, other transport-based proposed mechanism for the density limit in stellarators cannot be ruled-out. Transition from the bell-type, peaked profile into the broader, dome-type one can be achieved by external perturbation. Thus, and depending on wall recycling conditions, the injection of a short pulse of hydrogen can induce the transition, in a reversible (small pulse) or irreversible (large pulse) way. Examples of these types of transition are given in Fig. 6.

5. Energy Confinement

Figure 7 shows the evolution of plasma energy content as a function of the average electron density for different wall scenarios, gas species and plasma profiles. Preliminary data for plasmas under NBI heating with the two available sources are also included. Several features clearly appear from the figure. First, the range of available data extends to larger densities in the Li wall cases as compared to the B ones. This is a direct consequence of the lower threshold for plasma collapse existing in the later case. Global energy confinement times were obtained from the diamagnetic loop diagnostic after correction for the plasma current. Total injected power by the NBI system was measured by calorimetry. Total radiation was also taken into account for the available power coupled to the plasma. For the overlapping region ($n_e < 4 \times 10^{19} \text{ m}^{-3}$) confinement times, evaluated at the maximum of W_{dia} , im-

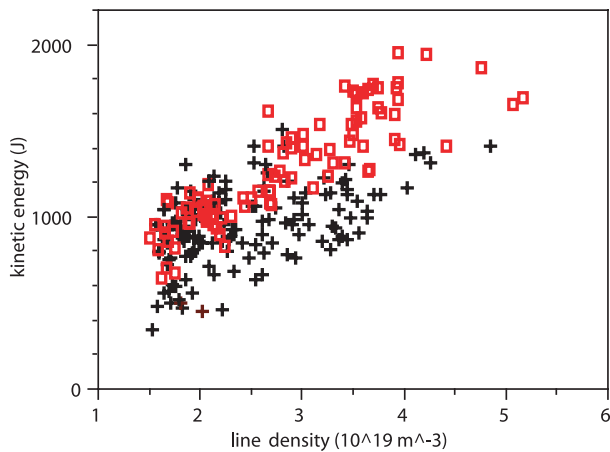


Fig. 7 Plasma energy content versus line density for B (black pluses) and Li (red squares) coated-wall discharges in plasmas heated with only one NBI.

prove from the B to the Li wall scenario. A strong dependence of t_E with $\langle n_e \rangle$ was deduced at least from the Li-wall scenarios, with t_E up to 20 ms. This enhancement of energy confinement with density is beyond that expected from usual scaling laws for stellarators [22] and accurate analysis is underway to isolate changes in this parameter that could be associated to bifurcations into enhanced modes. Some evidences on the presence of such bifurcations are provided through the conspicuous ELMy behaviour in the $H\alpha$ signals observed under NBI operation under some circumstances not clearly understood until now. A periodic oscillation in the edge parameters, with sharp bursts of less than 300 ms duration and a repetition rate of a few kHz, between two defined levels takes place at given line average density values and magnetic configuration. They are quickly followed by the generation of cold pulses which propagate in a ballistic time scale from a region located at ~ 4 -5 cm inside the LCFS in both directions. This plasma edge activity is correlated with important changes in the broadband density and electrostatic fluctuation levels at the edge, as detected by the reflectometer (in the density gradient region) and Langmuir probe (region around the LCFS) diagnostics, thus suggesting the presence of a transition to a confinement-enhanced regime. The characteristics of this regime and the requirements for its achievement are presently under investigation.

6. Conclusions

In the last year, the TJ-II has been operated under lithium-coated wall conditions, the first time that this

technique has ever been applied to a stellarator. Very encouraging results in terms of density control, plasma reproducibility and confinement characteristics have been obtained, dramatically enlarging the operational window of the machine even when only partial wall coverage with Li was achieved. NBI heated plasmas under stationary conditions have been produced up to record central densities of $8 \times 10^{19} \text{ m}^{-3}$, with no sign of local thermal collapse under the limited NBI power available during the campaign. Two different types of plasma profiles were recorded, with different behaviour respect to impurity accumulation. Strong ELM-type activity has been detected, in close correlation to fluctuation suppression at the edge and enhanced confinement.

Acknowledgements

This work was partially financed by the Spanish Ministry of Science and Innovation under project ENE2006-14577-CO4-CO3/FTN.

- [1] H. Wobig, *Plasma Phys. Control. Fusion* **42**, 931 (2000).
- [2] K. McCormick *et al.*, *Phys. Rev. Lett.* **89**, 015001 (2002).
- [3] O. Motojima *et al.*, *Phys. Rev. Lett.* **97**, 055002 (2006).
- [4] M.A. Ochando *et al.*, *Nucl. Fusion* **37**, 225 (1997).
- [5] Y. Takeiri *et al.*, *Plasma Phys. Control. Fusion* **42**, 147 (2000).
- [6] R. König *et al.*, *Fusion Sci. Technol.* **46**, 152 (2004).
- [7] K. Nishimura *et al.*, *J. Nucl. Mater.* **337-339**, 431 (2005).
- [8] A. Komori *et al.*, *J. Nucl. Mater.* **390-391**, 232 (2009).
- [9] J.N. Brooks *et al.*, *J. Nucl. Mater.* **337-339**, 1053 (2005) and refs. therein.
- [10] S. V. Mirnov *et al.*, *Plasma Phys. Control. Fusion* **48**, 821 (2006) and refs. therein.
- [11] V. Pericoli-Ridolfini *et al.*, *Plasma Phys. Control. Fusion* **49**, S123 (2007).
- [12] L.E. Zakharov *et al.*, *J. Nucl. Mater.* **363-365**, 453 (2007).
- [13] R. Majeski *et al.*, *Phys. Rev. Lett.* **97**, 075002 (2006).
- [14] J. Sánchez *et al.*, *Nucl. Fusion* **47**, S677 (2007).
- [15] F.L. Tabarés *et al.*, *J. Nucl. Mater.* **266-269**, 1273 (1999). Also, D. Tafalla *et al.*, *ibid.* **290-293**, 1195 (2001).
- [16] J. Sánchez *et al.*, *J. Nucl. Mater.* **390-391**, 852 (2009).
- [17] F.L. Tabarés *et al.*, *Plasma Phys. Control. Fusion* **43**, 1023 (2001).
- [18] M.A. Pedrosa *et al.*, *Plasma Phys. Control. Fusion* **49**, B303 (2007).
- [19] F.L. Tabarés *et al.*, "Impact of Lithium-coated walls on plasma performance in the TJ-II stellarator", Proc. 16th Intl. Stell/Hel Workshop 2007. Toki, Gifu, Japan, Oct. 15-19, 2007, I-20.
- [20] J. László and W. Eckstein, *J. Nucl. Mater.* **184**, 22 (1991).
- [21] A. Weller *et al.*, Report JET-IR-(87), 10 (1997).
- [22] H. Yamada *et al.*, *Nucl. Fusion* **45**, 1684 (2005).